FRONTIERS OF PHYSICS

RESEARCH ARTICLE
Volume 19 / Issue 4 / 42205 / 2024

Generation and characterization of customized Laguerre–Gaussian beams with arbitrary profiles

Chengyuan Wang[1,*,†], Yun Chen[1,2,*], Jinwen Wang[1], Xin Yang[1], Hong Gao[1,‡], Fuli Li[1]

1 Ministry of Education Key Laboratory for Nonequilibrium Synthesis and Modulation of Condensed Matter, Shaanxi Province Key Laboratory of Quantum Information and Quantum Optoelectronic Devices, School of Physics, Xi'an Jiaotong University, Xi'an 710049, China
2 Department of Physics, Huzhou University, Huzhou 313000, China
*These authors contributed equally to this work.
Corresponding authors. E-mail: †wcy199202@gmail.com, ‡honggao@mail.xjtu.edu.cn
Received October 10, 2023; accepted February 1, 2024

ABSTRACT

We experimentally demonstrate the generation of customized Laguerre–Gaussian (LG) beams whose intensity maxima are localized around any desired curves. The principle is to act with appropriate algebraic functions on the angular spectra of LG beams. We characterize the propagation properties of these beams and compare them with non-diffraction caustic beams possessing the same intensity profiles. The results manifest that the customized-LG beams can maintain their profiles during propagation and suffer less energy loss than the non-diffraction caustic beams, and hence are able to propagate a longer distance. Moreover, the customized-LG beam exhibits self-healing ability when parts of their bodies are blocked. This new structure beam has potential applications in areas such as optical communication, soliton routing and steering, and optical tweezing.

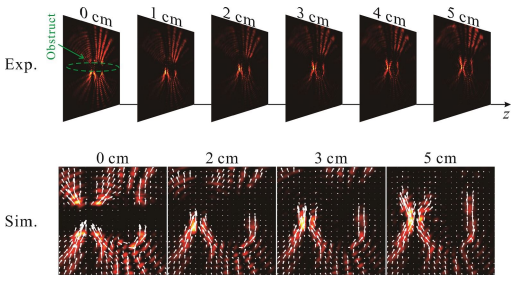

Keywords light manipulation, wave propagation, invariant optical fields

1 Introduction

Structure lights with customized intensity, phase, and polarization distributions [1, 2] have promoted the development of fundamental physics [3], optical trapping [4–6], imaging [7], optical communications [8, 9], and light–matter interactions [10–15], etc. Hermite–Gaussian (HG) beam [16], Laguerre–Gaussian (LG) beam [17], and Ince–Gaussian beam [18, 19] are three representative structure lights, which are the solutions of the paraxial wave equation under Cartesian, polar, and elliptical coordinates, respectively. These beams can remain their transverse profiles unchanged for about one Rayleigh length propagation, but suffer from an overall scaling of light spot due to diffraction. In 1987, by solving the Helmholtz equation in circular coordinates, Durnin [20] proposed a well-known non-diffracting beam, namely the Bessel beam, whose transverse structures neither deform nor expand over a significant propagation distance. However, an ideal Bessel beam with infinite energy is inaccessible practically. Thus in most realistic experiments, the Bessel beam is apodized to a Bessel–Gaussian (BG) beam [21–23] that can be approximated as non-diffracting. Alternatively, some other forms of non-diffracting beams, e.g., Mathieu beam [24] and Weber beam [25], can be obtained by extending the frame for solving the wave equation in elliptic and parabolic coordinates.

The above conventional non-diffracting beams have fixed, relatively simple transverse intensity distributions due to the limited classes of light fields, which in turn astricts their usefulness. To overcome this, several productive ways have been proposed [15, 26–28] to

Higher Education Press

https://doi.org/10.1007/s11467-024-1426-3

generate various types of non-diffracting or propagation-invariant beams, and most of them are based on spatial spectrum engineering techniques. It should be noted that the earliest related research can be traced back to the 1990s, in which the spiral-type beam in the form of arbitrary curves was put forward [29, 30] and later proved to be a class of caustic beam with propagation-invariant and resistance to perturbation [31]. As another representative example of customizing complex caustic beam, in 2020 Zannotti *et al.* [32] constructed arbitrary-shaped non-diffracting caustic beams through careful amplitude and phase modulation of the Bessel beam in Fourier space, also known as the Bessel pencil method. This method utilizes the most localized propagation-invariant light spot, namely a 0th-order Bessel beam, as a "pencil" to draw the desired beam along a preset curve. Shortly thereafter, Mendoza-Hernández [33] theoretically proposed that by acting an algebraic function on an LG beam in Fourier space, a new structured beam similar to the non-diffracting caustic beam can also be generated, and importantly, such a beam can preserve its profile a longer propagation distance than the non-diffracting caustic beam. Nevertheless, this work does not extend to generating arbitrarily shaped beams and yearning for experimental realization.

In this paper, we experimentally generate customized-LG beams with any desired shapes. The rationale is based on tailoring the LG beams in Fourier space by algebraic functions [33–35], which are constructed using the Bessel pencil method. To assess the propagation properties of the customized-LG beams, we also generate non-diffracting customized-BG beams [32] with the same transverse profiles for peer comparison. The experimental results show that the customized-LG beams can maintain their profiles during propagation and suffer less energy loss than the customized-BG beams, and hence can propagate a longer distance. Moreover, the self-healing ability of the customized-LG beam is also verified.

2 Principles

We first introduce the underlying principle. When a linear differential operator $\hat{\mathcal{A}}$ acts on an appropriate seed beam $U_0(r,z)$, a new customized beam $U(\boldsymbol{r},z)$ can be obtained with a complex transverse shape [33, 34] or on-demand trajectory [28, 36]. Such a transformation process can be expressed as

$$U(\boldsymbol{r},z)=\hat{\mathcal{A}}U_0(r,z), \tag{1}$$

where $\boldsymbol{r}=(x,y)$ is the transverse coordinate. Using the Fourier transform $\mathcal{F}$ and inverse Fourier transform $\mathcal{F}^{-1}$, Eq. (1) can be further written as

$$U=\mathcal{F}^{-1}\left\{\mathcal{F}\left\{\hat{\mathcal{A}}U_0\right\}\right\}=\mathcal{F}^{-1}\left\{\mathcal{A}\mathcal{F}\left\{U_0\right\}\right\}=\mathcal{F}^{-1}\left\{\mathcal{A}\tilde{U}_0\right\}, \tag{2}$$

where $\mathcal{A}$ is an algebraic function corresponding to the operator $\hat{\mathcal{A}}$ in Fourier space [34], $\tilde{U}_0$ is the Fourier transform of U_0 and can be optically obtained by a lens focusing process. The transformation process described in Eq. (2) can be physically realized by the setup shown in Fig. 1(a).

Since we focus on the seed of an LG beam and derive a collection of customized-LG beams based on the theory above, it is convenient to work with the expression of seed LG at the plane $z=0$

$$LGU_0=C_{\mathrm{LG}}L_p^{|0|}\left[\frac{2r^2}{\omega_{kt}^2(0)}\right]\exp\left[-\frac{r^2}{\omega_{kt}^2(0)}\right], \tag{3}$$

where C_{LG} is a constant coefficient, $L_p^{|0|}$ is the Laguerre polynomial with p being the radial order and azimuthal order $l=0$, $\omega_{kt}(0)=\omega_0/(2\sqrt{2N})$ with ω_0 being the input Gaussian beam waist and $N=p+1/2$. It should be emphasized that when $p\gg 1$, the LG beam can be regarded as a quasi propagation-invariant beam comparable to the BG beam. Thereupon, to evaluate the propagation characteristic of the customized-LG beams, we also generate customized-BG beams with similar shapes, i.e., a conventional light field with non-diffraction properties, for comparison. In general, the seed BG beam can be expressed by

$$BU_0=C_{\mathrm{B}}J_0\left(k_t r\right)\exp\left(-\frac{r^2}{\omega_{\mathrm{B}}^2}\right), \tag{4}$$

where C_{B} is a constant, $J_0(\cdot)$ is the zeroth order Bessel function of the first-kind, k_t is the transverse component of the wave vector $k=2\pi/\lambda$, ω_{B} is the waist of the BG beam [37]. Note that, the requirements for an LG beam to behave similarly to a BG beam should be $w_{\mathrm{B}}=\sqrt{2N}w_0$ and $k_t=2\sqrt{2N}/w_0$ [37], then the two beams have the same maximum propagation distance $z_{\max}=kw_0^2/2$ within which their spatial structure does not undergo obvious deformation during propagation. Interestingly, these relations are also often used to produce the perfect LG beam whose spot size does not change with its orbital angular momentum [38, 39].

The generation of several types of customized-LG beams, such as astroid-LG and deltoid-LG beams, have been theoretically proposed before [33] and verified in our experiments (see the Electronic Supplementary Material for details). Extending it to customizing arbitrary-shaped LG beams is somewhat challenging, mainly because it is difficult to construct the corresponding algebraic function $\mathcal{A}$. Inspired by the formal similarity between the LG and BG beams, we found that the Bessel-pencil method could also be utilized to construct complex customized-LG beams. The algebraic function of such a beam can be constructed by

$$\mathcal{A}=\int_a^b\exp\left[-\mathrm{i}k_t\boldsymbol{r}_{\mathrm{c}}(\tau)\cdot\boldsymbol{u}(\varphi)+\mathrm{i}\gamma_{\mathrm{B}}(\tau)\right]\mathrm{d}\tau, \tag{5}$$

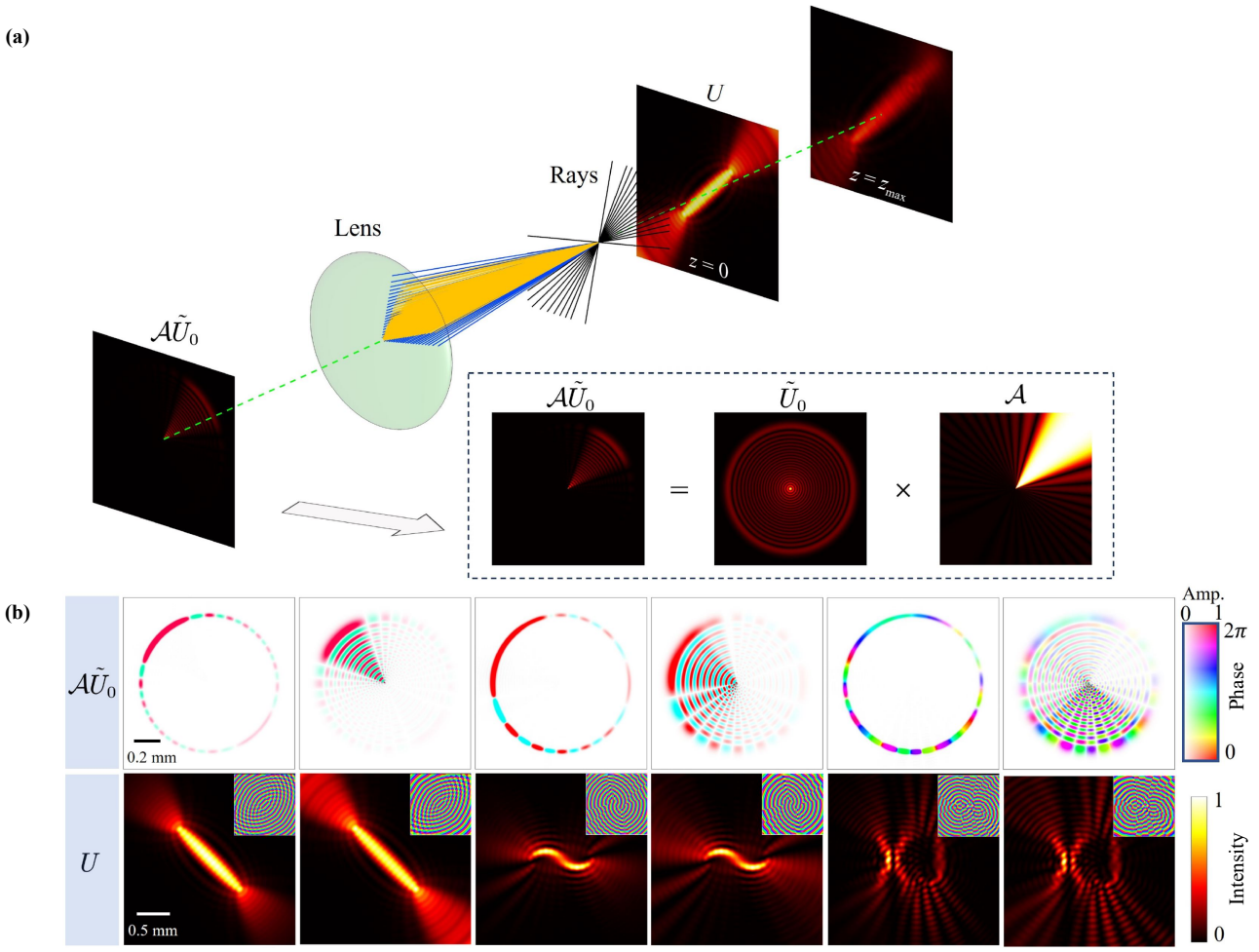

Fig. 1 **(a)** Schematic diagram of generating customized-LG beams. **(b)** Intensity and phase distribution of modulated spatial spectrum $\mathcal{A}\tilde{U}_0$ (first row) and the corresponding customized beams U (second row) with shapes of "sheet", "sinusoid", and "XJ", respectively. Note that two types of seed beams are used here, with columns 1, 3, and 5 corresponding to BG beam and columns 2, 4, and 6 corresponding to LG beam.

where $\boldsymbol{r}_c = (x_c, y_c)$ is the transverse coordinate along the desired curve, $\boldsymbol{u}(\varphi) = (\cos\varphi, \sin\varphi)$ is a unit vector related to the azimuthal angle, and τ is the arc length of the curve, and a/b is the head/tail of the curve. $\gamma_B(\tau)$ is a phase term growing with the curve's arc length τ, which can be obtained by

$$\gamma_B(\tau) = k_t \int_0^{\tau} |\boldsymbol{r}_c'(s)|\,\mathrm{d}s. \tag{6}$$

Based on the theory above we can obtain an arbitrary customized beam with an LG-seed or a BG-seed. For instance, we integrate Eq. (5) along three designed curves, i.e., "sheet", "sinusoid", and letters "XJ", and obtain the corresponding spatial angular spectrum modulation, and then obtain three kinds of customized-LG and customized-BG beams by Fourier transform, as shown in Fig. 2(b). For convenience, the sheet-shaped beam customized by LG or BG is abbreviated as LG/BG-sheet, while LG/BG-sine and LG/BG-XJ are named in the same way. The first row manifests that $\mathcal{A}$ acts as a phase and amplitude modulator on the angular spectrum, obtained by simulating the focusing process through a lens with $f = 20$ cm, of the two seed beams, whose parameters are set as $p = 20$, $w_0 = 0.2$ mm, $\omega_B = \sqrt{2(p+1/2)}\omega_0 = 1.3$ mm and $k_t = 2\sqrt{2(p+1/2)}/\omega_0 = 6.4 \times 10^4$ m^{-1}, such that they have similar intensity distribution and the same maximum propagation distance of $z_{max} = kw_0^2/2 = 16$ cm. The second row of Fig. 2(b) exhibits the intensity and phase distributions of the corresponding customized-BG and customized-LG beams. It can be observed that using the same algebraic function, the shapes of customized-BG beam and customized-LG beam are almost the same with the peripheral sideband ignored, and their intensity maxima are indeed localized around the preset curve. Essentially, the customized beams can be approximately regarded as an ordered coherent superposition of the seed beams, and therefore possess some properties, such as propagation

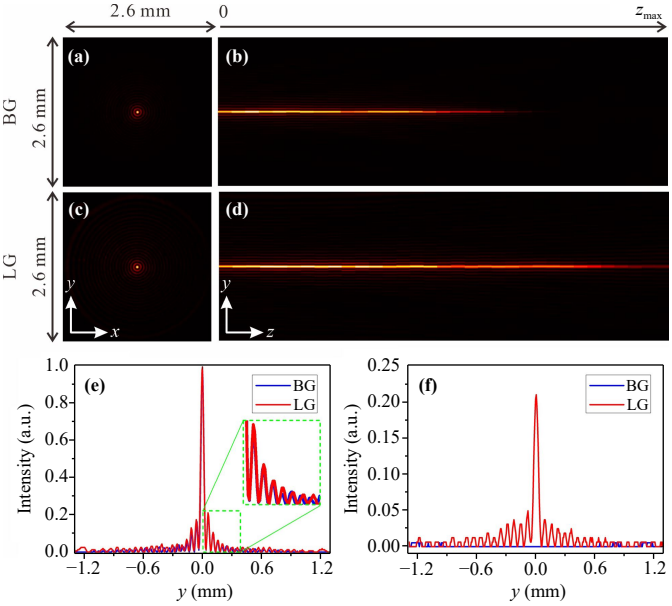

Fig. 2 Intensity distributions of the experimentally generated **(a)** BG and **(b)** LG beams. **(b, d)** are the beams' sectional propagation trajectories from $z = 0$ to $z = z_{max} = 16$ cm, and **(e, f)** are the intensity profiles of the two beams in the central region at propagation distances of $z = 0$ and $z = 16$ cm, respectively.

invariance and self-healing properties, of the corresponding seed beams, which we will focus on verifying experimentally in the following.

3 Experimental results and discussion

The detailed experimental configuration is given in the supplementary material. Given that the seed beam determines the propagation characteristics of customized beams, the propagation evolution of the seed beams in free space are firstly investigated. The parameters used here are completely consistent with those in Fig. 1.

Figures 2(a) and (c) show the intensity distributions of the seed BG and LG beams, Figs. 2(b) and (d) are the beams' sectional propagation trajectories from $z = 0$ to $z = z_{max}$, and Figs. 2(e) and (f) are the intensity profiles of the two beams in the central region at propagation distances of $z = 0$ and $z = z_{max}$, respectively. As can be seen that the two beams have nearly the same intensity distribution at $z = 0$ as expected. During propagation, the BG beam maintains its overall profile but its intensity attenuates quickly whereas the LG beam maintains its intensity profile much better but suffers slight broadening, e.g., at $z = z_{max}$ the BG is almost dissipated while the intensity maximum of the LG beam keeps to 21% of its original. This striking comparison indicates that compared with the customized-BG beam, the customized-LG beams suffer less intensity dissipation during long-distance propagation.

Next, the propagation of the three customized-LG/BG beams exhibited in Fig. 1 are studied experimentally in comparison. As shown by intensity volume in Fig. 3, the transverse intensities of the customized-BG beams decrease dramatically during propagation and are almost invisible at $z = z_{max}$. In contrast, the intensities of the customized-LG beams attenuate much slower and are still recognizable at the farthest distance. This result can be easily inferred from the conclusion obtained in Fig. 2, and is basically consistent with the theoretical simulation given in the supplementary. In addition, two noticeable phenomena are observed from Fig. 3. The first is the non-uniform attenuation of the customized beams during their propagation, even for the symmetrically distributed sheet beams. This is mainly because the transverse intensity and phase structure of the customized beams, "drawn" by the two seed beams, are not exactly symmetric about the origin, and the superimposed seed beams will inevitably interfere with each other during propagation. The second is that the diffraction of LG leads to slight distortion of the customized-LG beam, especially for the beams with complex structure [see Fig. 3(f)]. Nevertheless, this shape change does not significantly alter its original profile, and more importantly its overall intensity is well maintained compared to the customized-BG beam.

For quantitative analysis, we extract the intensity summation of each pattern and plot the total intensity variation against z, as shown in Figs. 3(g)–(i). One can find that in all cases given, the intensity of customized-LG is much higer than that of customized-BG beam after long-distance propagation. At $z = z_{max}$, the former still retains about 40% of its original while the latter is reduced to about 10%. Moreover, to assess the similarity between the transverse intensity distribution propagating to distance z (labeled as I_z) and the original transverse intensity distribution I_0, we use the normalized two-dimensional cross-correlation function which is simply defined as

$$\gamma(z) = \frac{I_0 * I(z)}{\sigma_{I_0}\sigma_{I(z)}}, \tag{7}$$

where $I_0 * I(z)$ denotes the cross-correlation function between I_0 and $I(z)$, σ_{I_0} and $\sigma_{I(z)}$ are standard deviations of the respective intensities. The maximum value of $\gamma(z)$ in each longitudinal position z is shown with an asterisk in Figs. 3(g)–(i) to represent the degree of correlation between I_z and I_0. Evidently, the correlation has a maximum value of 1 at $z = 0$ and decreases with the increase of z due to non-uniform transverse intensity attenuation and subtle distortion of the light field structure. For the light with simpler designed shape, e.g., "sheet" and "sinusoid" shaped beams, this decrease occurs more slowly, as can be seen by comparing Figs. 3(g) and (h), implying that they have a better

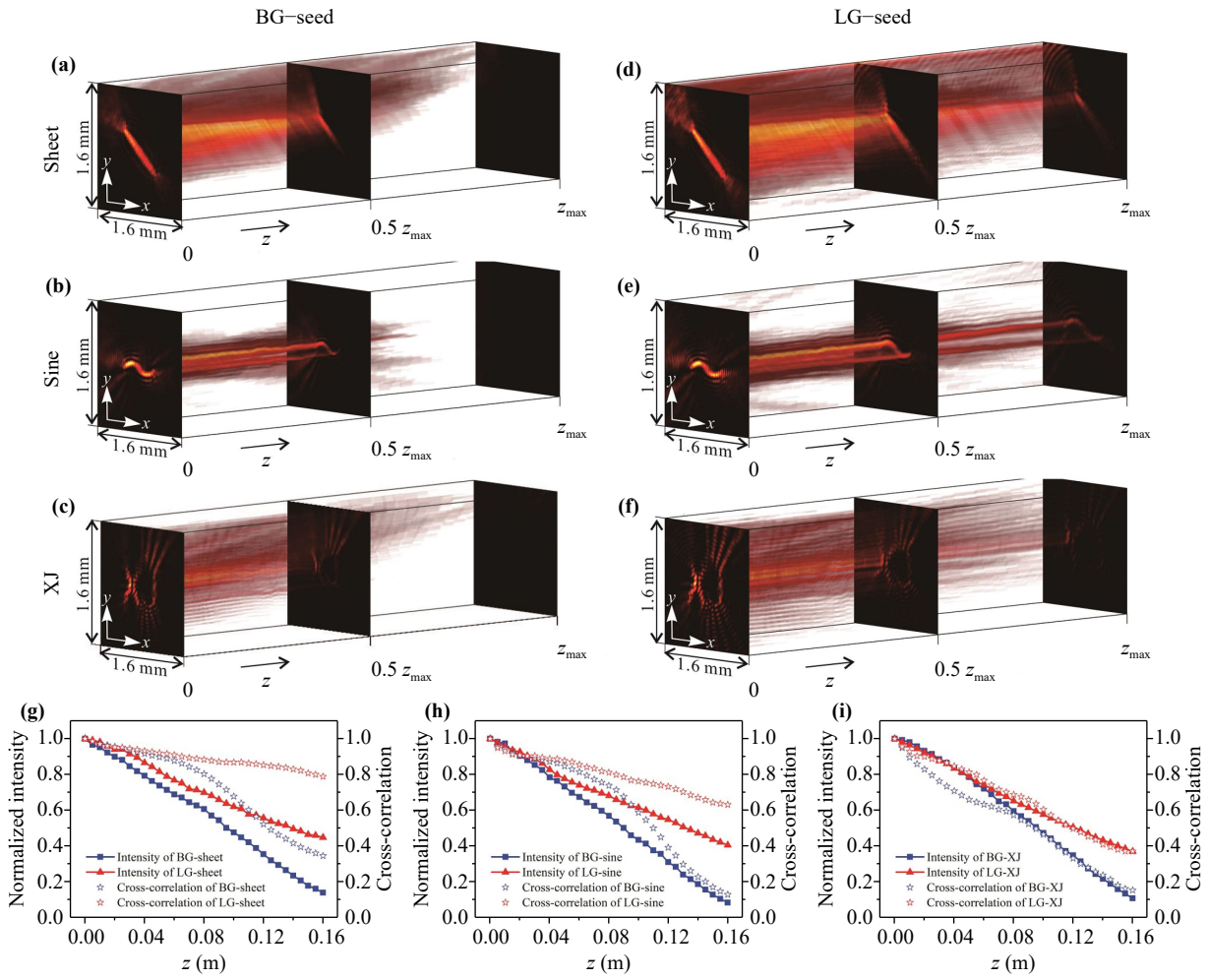

Fig. 3 Experimental obtained normalized intensity volume for **(a–c)** customized-BG and **(d–f)** customized-LG beams. **(g–i)** Intensity and cross-correlation function variations against z of the customized-BG and customized-LG beams.

performance in propagation invariability. On the other hand, for a specific target shape, the customized-LG beam has a higher correlation value than that of the customized-BG beam, especially at $z = z_{max}$, where the correlation difference between the two is up to about 50%. Note that this difference is mainly due to the fact that the transverse intensity of the customized-LG decays more uniformly and slowly, but on the other side, the shape distortion of the complex structured beam (such as LG-XJ) caused by the diffraction of LG will reduce this correlation gap, as can be found in Fig. 3(i). Even so, on the whole, the correlation value for customized-LG beam drops much slower than the customized-BG beam, especially over a distance of $0.5z_{max}$.

Finally, since it has been proved that the multi-ringed LG beam possesses the self-healing characteristic, here we further study whether the customized-LG beams heritage this characteristic. To this end, an obstruct is used to block parts of LG-XJ beam at $z = 0$. The evolution of the blocked beam at different propagation distances is displayed in Fig. 4(a). It is obvious that the occluded parts are almost restored at a propagation distance of 4 cm. The corresponding theoretical simulation, shown in Fig. 4(b), agrees well with the experimental result. The transverse energy flow (indicated by white arrows) is also calculated by introducing the time-averaged Poynting vector under the paraxial approximation:

$$\langle \boldsymbol{S} \rangle = \frac{\mathrm{i}}{2} ck\epsilon_0 (\psi^* \nabla \psi - \psi \nabla \psi^*), \tag{8}$$

where c is the speed of light in vacuum, ϵ_0 is the vacuum permittivity, ψ denotes the transverse light field and $*$ represents the complex conjugation item. The calculation manifests that the energy flux of the beam always flows along the customized curve. Consequently, the energy of the unoccluded region will continuously fill the occluded region and enable the beam to heal itself. Such an intriguing property may promote the application of customized-LG beams in a variety of complex environments.

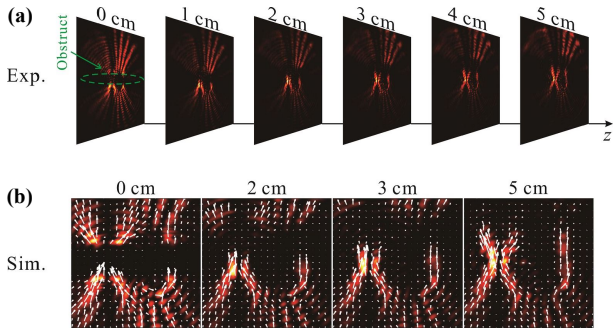

Fig. 4 Self-healing process of the "XJ" shaped customized-LG beam. The first row is the experiment result and the second row is the corresponding theoretical simulation.

4 Conclusion

In summary, we experimentally generate a series of customized-LG beams that can present any desired high-intensity distributions. The key ingredient is based on tailoring the angular spectrum of the LG beam by an algebraic function, which is constructed using the Bessel-pencil method. We also generate some non-diffraction caustic beams that possess the same intensity profiles with the customized-LG beams for comparison. The results show that the customized-LG beams can maintain their profiles and suffer less energy loss than the non-diffraction caustic beams and hence can propagate a longer distance. Moreover, the self-healing ability of the customized-LG beam is further verified, which agrees well with the theory and validates the excellent performance of the customized-LG beam during propagation. This new phyletic structure beam could find broad applications in areas such as optical communication, spatial soliton control, optical tweezing and trapping.

Declarations The authors declare that they have no competing interests and there are no conflicts.

Electronic supplementary materials The online version contains supplementary material available at https://doi.org/10.1007/s11467-024-1426-3 and https://journal.hep.com.cn/fop/EN/10.1007/s11467-024-1426-3.

Acknowledgements This work was supported by the National Natural Science Foundation of China (NSFC) (Nos. 12104358, 12104361, and 92050103) and Shaanxi Fundamental Science Research Project for Mathematics and Physics (No. 22JSZ004).

References

1. H. Rubinsztein-Dunlop, A. Forbes, M. V. Berry, M. R. Dennis, D. L. Andrews, M. Mansuripur, C. Denz, C. Alpmann, P. Banzer, T. Bauer, E. Karimi, L. Marrucci, M. Padgett, M. Ritsch-Marte, N. M. Litchinitser, N. P. Bigelow, C. Rosales-Guzmán, A. Belmonte, J. P. Torres, T. W. Neely, M. Baker, R. Gordon, A. B. Stilgoe, J. Romero, A. G. White, R. Fickler, A. E. Willner, G. Xie, B. McMorran, and A. M. Weiner, Roadmap on structured light, *J. Opt.* 19(1), 013001 (2016)
2. A. Forbes, M. de Oliveira, and M. R. Dennis, Structured light, *Nat. Photonics* 15(4), 253 (2021)
3. A. Hansen and T. Justin, Schultz, and Nicholas P Bigelow, Singular atom optics with spinor Bose–Einstein condensates, *Optica* 3(4), 355 (2016)
4. Y. Yang, Y. Ren, M. Chen, Y. Arita, and C. Rosales-Guzmán, Optical trapping with structured light: A review, *Adv. Photonics* 3(3), 034001 (2021)
5. E. Otte and C. Denz, Optical trapping gets structure: Structured light for advanced optical manipulation, *Appl. Phys. Rev.* 7(4), 041308 (2020)
6. J. Baumgartl, M. Mazilu, and K. Dholakia, Optically mediated particle clearing using airy wavepackets, *Nat. Photonics* 2(11), 675 (2008)
7. A. Forbes, M. de Oliveira, and M. R. Dennis, Light-sheet microscopy using an airy beam, *Nat. Methods* 11(5), 541 (2014)
8. J. P. Torres, Multiplexing twisted light, *Nat. Photonics* 6(7), 420 (2012)
9. A. E. Willner, K. Pang, H. Song, K. Zou, and H. Zhou, Orbital angular momentum of light for communications, *Appl. Phys. Rev.* 8(4), 041312 (2021)
10. J. Wang, F. Castellucci, and S. Franke-Arnold, Vectorial light–matter interaction: Exploring spatially structured complex light fields, *AVS Quantum Sci.* 2(3), 031702 (2020)
11. Z. K. Wu, H. Guo, W. Wang, and Y. Z. Gu, Evolution of finite energy airy beams in cubic–quintic atomic vapor system, *Front. Phys.* 13(1), 134201 (2018)
12. F. Niu, H. Zhang, J. Yuan, L. Xiao, S. Jia, and L. Wang, Photonic graphene with reconfigurable geometric structures in coherent atomic ensembles, *Front. Phys.* 18(5), 52304 (2023)
13. C. Wang, Y. Yu, Y. Chen, M. Cao, J. Wang, X. Yang, S. Qiu, D. Wei, H. Gao, and F. Li, Efficient quantum memory of orbital angular momentum qubits in cold atoms, *Quantum Sci. Technol.* 6(4), 045008 (2021)
14. Y. Chen, J. Wang, C. Wang, S. Zhang, M. Cao, S. Franke-Arnold, H. Gao, and F. Li, Phase gradient protection of stored spatially multimode perfect optical vortex beams in a diffused rubidium vapor, *Opt. Express* 29(20), 31582 (2021)
15. C. Wang, Y. Chen, Z. Jiang, Y. Yu, M. Cao, D. Wei, H. Gao, and F. Li, Experimental investigation of light storage of diffraction-free and quasi-diffraction-free beams in hot atomic gas cell, *Front. Phys.* 17(2), 22503 (2022)
16. Y. Wang, Y. Chen, Y. Zhang, H. Chen, and S. Yu, Generalised Hermite–Gaussian beams and mode transformations, *J. Opt.* 18(5), 055001 (2016)
17. L. Allen, M. W. Beijersbergen, R. J. C. Spreeuw, and J. P. Woerdman, Orbital angular momentum of light and the transformation of Laguerre–Gaussian laser modes, *Phys. Rev. A* 45(11), 8185 (1992)
18. M. A. Bandres and J. C. Gutiérrez-Vega, Ince–Gaussian beams, *Opt. Lett.* 29(2), 144 (2004)

19. Y. Yu, Y. Chen, C. Wang, J. Wang, Z. Sun, M. Cao, H. Gao, and F. Li, Optical storage of Ince–Gaussian modes in warm atomic vapor, *Opt. Lett.* 46(5), 1021 (2021)
20. J. Durnin, J. J. Miceli, and J. H. Eberly, Diffraction-free beams, *Phys. Rev. Lett.* 58(15), 1499 (1987)
21. M. McLaren, M. Agnew, J. Leach, F. S. Roux, M. J. Padgett, R. W. Boyd, and A. Forbes, Entangled Bessel–Gaussian beams, *Opt. Express* 20(21), 23589 (2012)
22. X. Chu, Q. Sun, J. Wang, P. Lü, W. Xie, and X. Xu, Generating a Bessel–Gaussian beam for the application in optical engineering, *Sci. Rep.* 5(1), 18665 (2015)
23. Z. Zhi, Q. Na, Q. Xie, B. Chen, Y. Li, X. Liu, X. Li, L. Wang, G. Lo, and J. Song, On-chip generation of Bessel–Gaussian beam via concentrically distributed grating arrays for long-range sensing, *Light Sci. Appl.* 12(1), 92 (2023)
24. J. C. Gutiérrez-Vega, M. D. Iturbe-Castillo, and S. Chávez-Cerda, Alternative formulation for invariant optical fields: Mathieu beams, *Opt. Lett.* 25(20), 1493 (2000)
25. M. A. Bandres, J. C. Gutiérrez-Vega, and S. Chávez-Cerda, Parabolic nondiffracting optical wave fields, *Opt. Lett.* 29(1), 44 (2004)
26. P. A. Sanchez-Serrano, D. Wong-Campos, S. Lopez-Aguayo, and J. C. Gutiérrez-Vega, Engineering of nondiffracting beams with genetic algorithms, *Opt. Lett.* 37(24), 5040 (2012)
27. S. López-Aguayo, Y. V. Kartashov, V. A. Vysloukh, and L. Torner, Method to generate complex quasinon-diffracting optical lattices, *Phys. Rev. Lett.* 105(1), 013902 (2010)
28. W. Yan, Y. Gao, Z. Yuan, Z. Wang, Z. C. Ren, X. L. Wang, J. Ding, and H. T. Wang, Non-diffracting and self-accelerating Bessel beams with on-demand tailored intensity profiles along arbitrary trajectories, *Opt. Lett.* 46(7), 1494 (2021)
29. E. Abramochkin and V. Volostnikov, Spiral-type beams, *Opt. Commun.* 102(3-4), 336 (1993)
30. E. Abramochkin and V. Volostnikov, Spiral-type beams: Optical and quantum aspects, *Opt. Commun.* 125(4-6), 302 (1996)
31. A. Volyar and Y. Akimova, Structural stability of spiral vortex beams to sector perturbations, *Appl. Opt.* 60(28), 8865 (2021)
32. A. Zannotti, C. Denz, M. A. Alonso, and M. R. Dennis, Shaping caustics into propagation-invariant light, *Nat. Commun.* 11(1), 3597 (2020)
33. J. Mendoza-Hernández, Customizing structured light beams with a differential operator, *Opt. Lett.* 46(20), 5232 (2021)
34. I. Martinez-Castellanos and J. C. Gutiérrez-Vega, Shaping optical beams with non-integer orbital-angular momentum: A generalized differential operator approach, *Opt. Lett.* 40(8), 1764 (2015)
35. J. Mendoza-Hernández, M. Szatkowski, M. F. Ferrer-Garcia, J. C. Gutiérrez-Vega, and D. Lopez-Mago, Generation of light beams with custom orbital angular momentum and tunable transverse intensity symmetries, *Opt. Express* 27(18), 26155 (2019)
36. T. Čižmár and K. Dholakia, Tunable Bessel light modes: Engineering the axial propagation, *Opt. Express* 17(18), 15558 (2009)
37. J. Mendoza-Hernández, M. L. Arroyo-Carrasco, M. D. Iturbe-Castillo, and S. Chávez-Cerda, Laguerre–Gauss beams versus Bessel beams showdown: Peer comparison, *Opt. Lett.* 40(16), 3739 (2015)
38. J. Mendoza-Hernández, M. Hidalgo-Aguirre, A. Inclán Ladino, and D. Lopez-Mago, Perfect Laguerre–Gauss beams, *Opt. Lett.* 45(18), 5197 (2020)
39. X. Liu, Y. E. Monfared, R. Pan, P. Ma, Y. Cai, and C. Liang, Experimental realization of scalar and vector perfect Laguerre–Gaussian beams, *Appl. Phys. Lett.* 119(2), 021105 (2021)